RSC Advances

PAPER

View Article Online
View Journal | View Issue

Cite this: *RSC Adv.*, 2022, **12**, 27633

Flame retardant chloroprene rubbers with high tensile strength and elongation at break *via* dual cross-linked networks

Jianliang Jiang,†[ab] Junxue Zhai,†[c] Lingxin Kong,[c] Dongqi Zhao[d] and Yakai Feng *[ab]

The tensile strength and elongation at break of rubbers are mutually restrictive factors. Design and preparation of chloroprene rubber (CR) with high tensile strength, high elongation at break and excellent flame retardancy at the same time is challenging. Melamine cyanurate (MCA) is for the first time discovered to be a reactive flame retardant for CR. The tensile strength of C-M36 (with 3 wt% ZnO and 36 wt% MCA) vulcanizate is 2.5 times that of C-M0 (only with 3 wt% ZnO) vulcanizate, while the elongation at break of C-M36 vulcanizate is 1.3 times that of ZnO cross-linked C-M0 vulcanizate. At the same time, the limiting oxygen index of C-M36 (39%) is 1.22 times that of C-M0 (32%). FTIR and the vulcanization tests confirm that the reaction between CR and cyanuric acid occurs under the catalysis of a base (melamine), and the cyanuric acid molecules are grafted onto the molecular chain of CR. Two types of crosslinking networks are formed in CR vulcanizate, namely the traditional covalent bond crosslinks and the triple hydrogen crosslinks formed between cyanuric acid and melamine. Thus, the flame-retardant CR/MCA vulcanizate with high strength and high elongation at break is obtained. This research will strongly promote the industrial application of CR.

Received 28th August 2022
Accepted 21st September 2022

DOI: 10.1039/d2ra05389f

rsc.li/rsc-advances

1 Introduction

Chloroprene rubber (polychloroprene or neoprene) is a traditional rubber synthesized by free radical polymerization of chloroprene (2-chloro-1,3-butadiene),[1,2] and can also be prepared by RAFT or RIFA reaction.[3,4] Due to excellent mechanical properties and flame retardant properties, chloroprene rubber (CR) presently finds wider application in automobiles, aircraft, protective layers of cables and wires, conveyor belts, V-belts, heat-resistant conveyor belts, chemical-resistant hoses and other fields.[5–10] Chloroprene is a monomer that was first used in the synthesis of chloroprene rubber at an industrial scale, and it is still used in the production of chloroprene rubber to this day.[11] Chlorine and C=C double bonds in the polymer chain endow CR with some basic properties. For example, the strong polarity in the carbon–chlorine bond increases the force between the polymer chains of CR, so CR has excellent mechanical properties and chemical stability. At the same time, the chlorine in the polymer chain makes the limiting oxygen index (LOI) of chloroprene rubber high. Combined with the use of a small amount of flame retardant, it is easy to design a CR vulcanizate with excellent flame retardant properties.[12,13] When designing the flame retardant CR vulcanizate by traditional methods, filler-type flame retardants are generally added, and the improvement of the flame retardant performance of the material often sacrifices the mechanical properties. Therefore, it is challenging to design and prepare CR with the high tensile strength, elongation at break, and excellent flame-retardant properties at the same time.

The ever-increasing demand for energy consumption and the pollution from energy access have put more pressure on the entire human society.[14–17] The traditional rubber vulcanization method consumes a lot of energy, and the vulcanization process is not friendly to the environment. Therefore, the green vulcanization method of rubber has become a research hotspot. ZnO/MgO particles were frequently used as CR vulcanizing agents,[6] as their vulcanization process has the advantages of low energy consumption, light environmental pollution, and little harm to operators. Tripathy *et al.*[18] proposed a vulcanization reaction mechanism between CR and MgO. Two C=C–C–Cl groups of CR react with MgO to form a C=C–C–O–C–C=C bond and $MgCl_2$. Peter Kovacic discovered the crosslinking reaction between CR and piperazine with elimination of hydrogen chloride.[19] Moreover, the use of lead oxide was also reported for

[a]*School of Chemical Engineering and Technology, Frontiers Science Center for Synthetic Biology, Key Laboratory of Systems Bioengineering (Ministry of Education), Tianjin University, Yaguan Road 135, Tianjin 300350, China. E-mail: yakaifeng@tju.edu.cn*

[b]*Frontiers Science Center for Synthetic Biology, Key Laboratory of Systems Bioengineering (Ministry of Education), Tianjin University, Yaguan Road 135, Tianjin 300350, China*

[c]*Key Laboratory of Rubber-Plastics of Ministry of Education/Shandong Province, School of Polymer Science & Engineering, Qingdao University of Science & Technology, 5 Zhengzhou Road, Qingdao 266042, China*

[d]*Tianjin Joaboa Technology Co., Ltd, No. 24 Road, Tianjin 301609, P. R. China*

† Jianliang Jiang and Junxue Zhai contributed equally to this work.

vulcanization, however, due to the environmental pollution of lead elements, this vulcanization method was rarely used in the industrial application of CR. Imidazole compounds were also reported in patents, but the mechanism of their vulcanization reaction of CR is not very clear.[20] The chlorine atom in the CR polymer chain makes the reactivity of the C=C bond and the carbon atom connected to the C=C bond (C=C–C–X, hydrogen or chlorine) different from that of the traditional rubber. Therefore, the traditional sulfur vulcanization method cannot vulcanize CR very well.[9]

Most of the crosslinks obtained by the existing CR vulcanization methods are covalent bonds, and the tensile strength and elongation at break of CR cannot be simultaneously improved. The dynamic bond crosslinking of rubber to achieve the simultaneous improvement of the tensile properties and elongation at break of the material has been reported in the literature.[21–24] Chen *et al.*[25] found that the tensile strength and elongation at break of PBMs cross-linked by dynamic bond (Fe^{2+}–pyrazine) were 2 times and 23 times higher than those of PBMs cross-linked by covalent bonds. Xie *et al.*[26] introduced Fe^{3+}–COOH coordination bonds into the hydrogel network of polyacrylic acid to form a double network structure and also achieved a significant improvement in the strength and elongation at break of the hydrogel. Inspired by the above literature, the primary goal of this paper is to find a dynamic crosslinking method for CR.

Melamine cyanurate (MCA) is a kind of green and environmentally friendly flame-retardant and its application in plastics has received more and more attention.[27–30] MCA is very stable within 300 °C, and decomposes above 600 °C.[31] Moreover, MCA is a nitrogen-based, intumescent flame retardant. The vulcanizate added with MCA has excellent flame-retardant properties, and low smoke density during combustion and rarely produces toxic and corrosive gases.[32–34] Traditionally, MCA is generally added to materials as an additive flame retardant. In the early exploratory test, we unexpectedly found that after the addition of MCA in CR, the vulcanization rate slowed down and the mechanical properties of the CR vulcanizate also changed significantly. After the detailed study, it was found that MCA could react with CR to form a network structure of dynamic bond crosslinking. Surprisingly, after adding zinc oxide and MCA to CR, with the addition of zinc oxide and MCA to CR, both covalent bonds and dynamic chemical bonds were formed in CR vulcanizate. Excitingly, the tensile strength and elongation at break of CR vulcanizate were improved at the same time and the flame retardancy of CR has also been significantly improved. In this work, we inadvertently discovered a new dynamic crosslinking method for CR, which provides a new strategy for the improvement of CR performance.

2 Experimental

2.1 Materials

Chloroprene rubber CR3221 was supplied by Chongqing Chang-shou Chemical Co., Ltd, China. Melamine cyanurate (MCA) was supplied by Qingdao Ouen Industrial Technology Co., Ltd, China. ZnO and other chemical reagents were obtained from Aladdin.

Table 1 Blend designations and compositions

	Sample ID					
Ingredient (phr)	C-M0	C-M3	C-M6	C-M12	C-M24	C-M36
CR	100	100	100	100	100	100
ZnO	3	3	3	3	3	3
MCA	0	3	6	12	24	36
Stearic acid	1	1	1	1	1	1

2.2 Preparation of flame retardant chloroprene rubbers

The X(S)K-160 double-roll mill was used for kneading. Firstly, the CR3221 rubber was put into the open mill and plasticized through the rolls for 5 times. Then, zinc oxide, MCA and stearic acid were added and mixed evenly. Finally, the roll distance was adjusted to 2 mm to produce rubber sheets. The vulcanization reaction tests were carried out after parking for 8 h.

The blend designations and compositions are shown in Table 1.

2.3 Measurement and characterization

The vulcanization characteristics were tested according to ASTM D2084-2001 using a Moving Die Rhometer GT-M2000-A (Gaotie Test Instruments Factory, China) at 170 °C.

The tensile properties of the samples were tested according to GB/T 528-2009 using a GT-AI-7000-S high temperature stretching machine with a speed of 500 mm min^{-1}, at 30 °C and 180 °C, respectively. The average value of three individual samples was recorded for each sample.

ATR-FTIR spectra were recorded on a VERTEX70 spectrometer. Samples were characterized by signal averaging 32 scans at a resolution of 4 cm^{-1} in the wavenumber range of 500–4000 cm^{-1}.

The friction coefficient of the samples was tested by the GT-7012-AF tester and the static and dynamic friction coefficients of the vulcanized rubber on the glass surface were determined according to GB/T 10006-2021. The average value of three individual samples was recorded for each sample.

The high-temperature aging tests were carried out in a GT-7017-E incubator and the aging condition was 200 °C × 2 h.

The limiting oxygen index of the samples were tested by HC-2 oxygen index tester. The tests were carried out according to the method of GB/T 2406.2-2009.

3 Results and discussion

3.1 The effect of MCA on the vulcanization characteristics of CR

The vulcanization data of the CR/MCA compound at 170 °C are showed in Table 2 and Fig. 1. The curve of scorch time (T_{10}) indicates that MCA content has little effect on the scorch time of CR/MCA. MCA content has a significant effect on the positive vulcanization time (T_{90}) of the CR/MCA and T_{90} increases monotonically with the increase of MCA content. Therefore, it

Table 2 Curing parameters of CR with MCA at 170 °C

Test items	Sample ID					
	C-M0	C-M3	C-M6	C-M12	C-M24	C-M36
T_{10}/min	0.64	0.70	0.66	0.62	0.61	0.63
T_{90}/min	8.40	10.25	10.75	11.30	13.02	16.03
M_L/dN m	0.36	0.42	0.46	0.48	0.56	0.62
M_H/dN m	6.13	6.30	6.52	7.50	8.67	10.06

can be inferred that besides of the familiar crosslinking reaction between zinc oxide and CR, there may also be a crosslinking reaction between CR and MCA.

As shown in Table 2 and Fig. 1, with the increase of MCA content, the minimum torque (M_L) increases slowly, but the maximum torque (M_H) increases significantly. The M_H of C-M36 is 1.64 times that of C-M0. It is generally believed that the value of M_H is positively related to the crosslinking density of rubber, so we can infer that MCA has indeed involved in the crosslinking reaction with CR.

MCA is formed by self-assembly of melamine and cyanuric acid through intermolecular hydrogen bond interactions (amino and carbonyl) and has a stable supramolecular structure (Fig. 2).[35] Under the catalysis of organic bases, the reaction of the N–H of cyanuric acid with C–Cl bond of small molecules can take place with a good yield (>90%), which has been reported in the literature.[36,37] The melting point of MCA is close to 350 °C, which is much higher than the vulcanization temperature of CR. During the vulcanization at 170 °C, the reaction between MCA and CR is heterogeneous (solid–liquid reaction). It can be speculated that a nucleophilic substitution reaction between the N–H group of the cyanuric acid (located at the interface of MCA crystal) and C–Cl bond of CR occurs under alkali catalysis (melamine), but the other two N–H groups of one cyanuric acid inside the MCA crystal could not react with the C–Cl bond of CR (Fig. 2), because of their triple hydrogen bonding. Therefore, a possible crosslinking reaction between CR and MCA is proposed (Fig. 3).

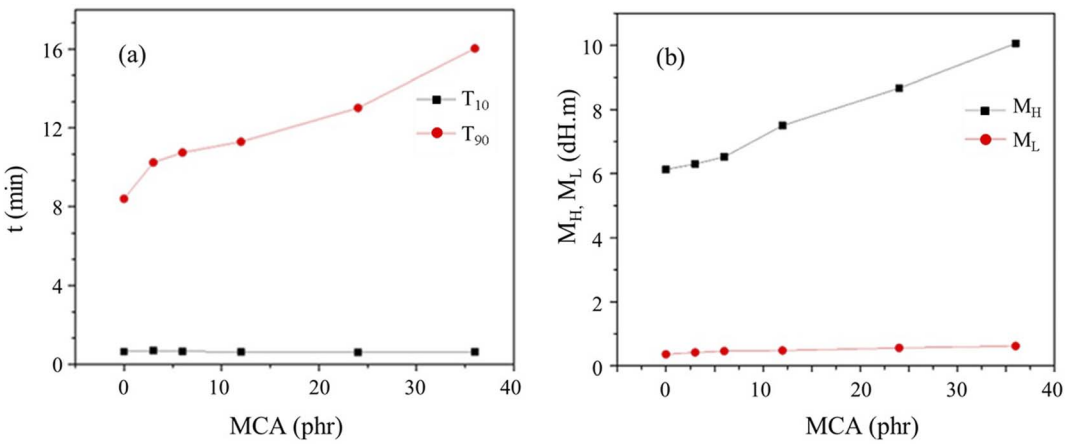

Fig. 1 The vulcanization data of CR/MCA. (a) t_{10}, t_{90} of CR/MCA, (b) M_H, M_L of CR/MCA.

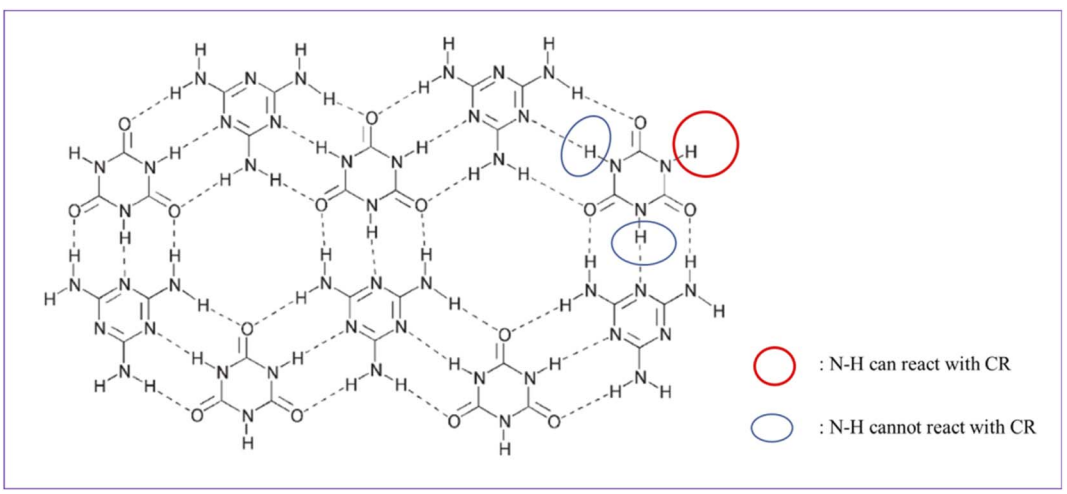

Fig. 2 A portion of the two-dimensional MCA network.

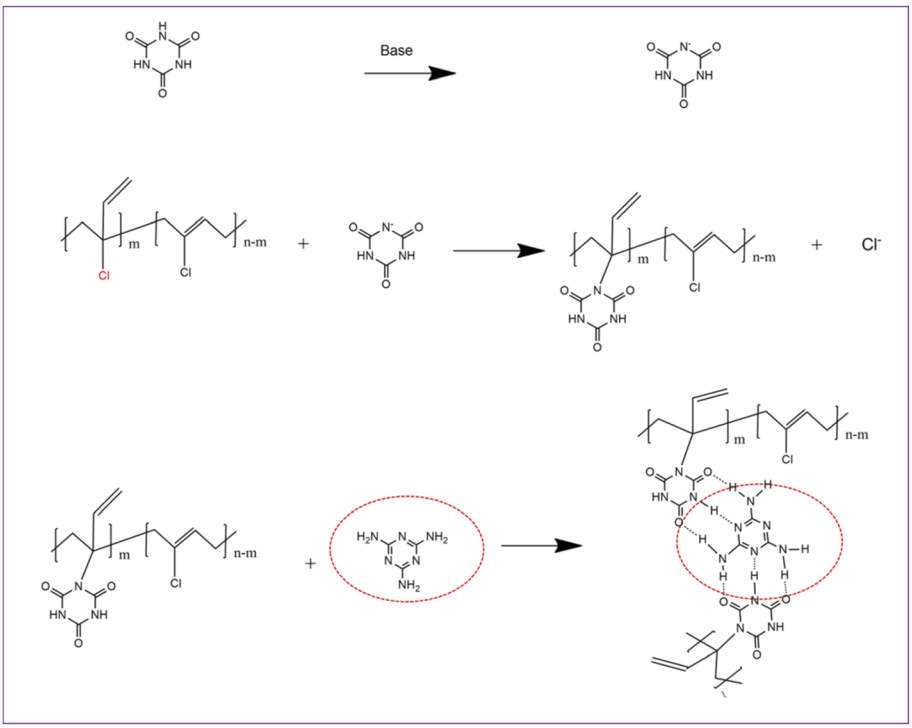

Fig. 3 Possible reactions between MCA and CR (inside the red ellipse, melamine molecules are confined to the surface of the MCA crystal).

3.2 FTIR characterization of CR/MCA

FTIR spectroscopy was used to further verify the reaction between MCA and CR. As shown in Fig. 3, the characteristic absorption peaks of CR (Fig. 4a) mainly include: 2916 cm^{-1} is assigned to the stretching vibration of C–H, 1659 cm^{-1} is assigned to the stretching vibration of C=C, 667 cm^{-1} is assigned to the stretching vibration of C–Cl. The characteristic absorption peaks of MCA (Fig. 4b) are consistent with those reported in the literature,[38] these characteristic peaks mainly include: 3374 cm^{-1}, 3235 cm^{-1} are the symmetric stretching vibration peak of N–H of melamine and cyanuric acid; 1531 cm^{-1} and 1443 cm^{-1} are the characteristic absorption peaks of triazine ring. 1778 cm^{-1} and 1731 cm^{-1} are the symmetric and asymmetric stretching peak of C=O.

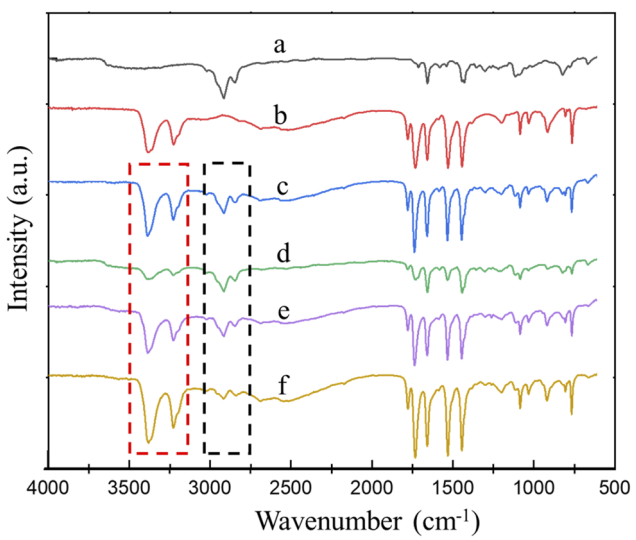

Fig. 4 ATR-FTIR spectra of different materials. (a) CR; (b) MCA; (c) CR/MCA; (d) CR/MCA (superimposed spectra of CR and MCA); (e) CR/MCA (aging, 200 °C × 2 h); (f) CR/MCA (aging, 200 °C × 2 h, then sanded).

The C=O absorption band of free cyanuric acid is exhibited at 1690 cm^{-1}.[39,40] Due to the triple hydrogen bonds between cyanuric acid and melamine, the C=O absorption band of MCA and CR/MCA is shifted to high wavenumber at 1778 cm^{-1} and 1731 cm^{-1}, respectively. This is due to the increase in stiffness of C=O arising from the formation of hydrogen bonding between melamine and cyanuric acid.[41,42] Unfortunately, only very small part of cyanuric acid (located at the edge of MCA crystal) could react with CR through nucleophilic substitution, which is difficult to be monitored by the intensity or shift of the carbonyl absorption peak.

The N–H absorption peak of free cyanuric acid is presented at 3427 cm^{-1}, while the N–H absorption band of free melamine is presented at 3427 and 3472 cm^{-1}.[41,42] Because of the triple hydrogen bond, the N–H absorption band of MCA and CR/MCA was shifted to low wavenumber at 3374 and 3235 cm^{-1}, respectively. Taking the C–H absorption peak at 2916 cm^{-1} of CR as the reference peak, the change of MCA content can be judged by the absorption peak height of N–H relative to that of C–H. As shown in Fig. 4c, the ATR-FTIR spectrum of CR/MCA vulcanizate shows the characteristic peaks of CR and MCA. Comparing with Fig. 4c and d, the absorption peak intensities of CR/MCA are higher than those calculated by content, the possible reason is that CR promotes the dispersion of MCA powder during the mixing and

vulcanization process. The particle size becomes smaller and the interface area increases. Therefore, the number of N–H on the MCA crystal interface increases.

Comparing with Fig. 4c and e, it can be found that the intensity of the N–H stretching vibration absorption peaks at 3374 cm^{-1}, 3235 cm^{-1} of CR/MCA vulcanizate further decreases after aging, while the absorption peak intensity of C–H bond at 2916 cm^{-1} is basically unchanged, indicating the N–H bond of cyanuric acid can react with the C–Cl bond of CR under the catalysis of melamine. Herein, MCA acts as both a reactant and a catalyst.

The influence of grinding on the surface of CR/MCA vulcanizate was further investigated (using sandpaper, with a grinding thickness of about 0.5 mm). Comparing with Fig. 4e and f, the intensity of N–H absorption peaks at 3374 cm^{-1}, 3235 cm^{-1} of CR/MCA vulcanizate after surface grinding is significantly higher than those of CR/MCA vulcanizate without surface grinding. The intensity of C–H absorption peak at 2916 cm^{-1} decreases significantly after surface grinding, because CR is easier to remove during the grinding process, the CR content decreases and the MCA content increases on the surface layer of the CR/MCA vulcanizate. This result is consistent with the results discussed in the CR friction coefficient section later.

3.3 Tensile properties of CR/MCA

The tensile properties of CR/MCA vulcanizates were tested at 30 °C and 180 °C, respectively. The tensile data of CR/MCA vulcanizates at 30 °C are shown in Table 3, it can be found that the tensile strength of CR/MCA vulcanizates at 25%, 100% and 300% fixed strain increases with an increasing MCA content. When the MCA content was 12 or 36 phr, the tensile strength and elongation at break of the CR/MCA vulcanizate are simultaneously improved. The tensile strength of C-M36 vulcanizate is 2.5 times that of zinc oxide cross-linked C-M0 vulcanizate, while the elongation at break of C-M36 vulcanizate is 1.3 times that of zinc oxide cross-linked C-M0 vulcanizate.

As shown in Table 3, the tensile strength of the C-M*x* vulcanizate decreases significantly at high temperature. The tensile strength of C-M*x* vulcanizate at 180 °C is 0.1–0.5 times that of C-M*x* vulcanizate at 30 °C. Mainly because the force between the polymer chains of CR decreases with increasing temperature. The tensile strength of C-M*x* vulcanizate increases with the increase of MCA content at 180 °C. The tensile strength of C-M36 vulcanizate is 3.2 times that of zinc oxide cross-linked C-M0 vulcanizate, while the elongation at break of C-M36 vulcanizates is 8.6 times that of zinc oxide cross-linked C-M0 vulcanizates.

For conventional vulcanizates, it is difficult to achieve simultaneous improvement in tensile strength and elongation at break. It can be seen from Table 3 that the tensile strength and elongation at break of the CR/MCA vulcanizate are both improved compared to the traditional zinc oxide vulcanized CR. During the stretching process, the triple H-bonding crosslinks in the CR/MCA vulcanizate play an important role in the stretching process. The crosslinking bonds of zinc oxide vulcanized CR are covalent bonds. Due to the uneven distribution of covalent bond crosslinks, the covalent crosslinking bonds at the stress concentration point are broken firstly, and the tensile strength and elongation at break cannot be increased at the same time (Fig. 5a). The CR/MCA vulcanizate contains both covalent crosslink bonds and triple hydrogen bond crosslinks. During the stretching process, the triple H-bonding crosslinks are first broken, which is conducive to the adjustment of the configuration of the CR molecular chains along the stretching direction. The generation of cyanuric acid on the side chain of the CR molecule can simultaneously form new triple H-bonding crosslinks with other nearby MCAs, thereby significantly improving the tensile strength and elongation at break of the CR/MCA vulcanizate (Fig. 5b). The tensile strength and elongation at break of CR/MCA vulcanizates at 180 °C are more significantly improved than those of CR/MCA vulcanizates at 30 °C. Probably because the high temperature is more conducive to the dissociation and recombination of triple H-bonding.

3.4 The effect of MCA on the static friction coefficient of CR/MCA

The CR vulcanizate samples are easily deformed during the test, resulting in the unstable test data. Therefore, the samples were

Table 3 Tensile properties of CR/MCA vulcanizates

	Samples					
Test items	C-M0	C-M3	C-M6	C-M12	C-M24	C-M36
At 30 °C						
Tensile strength, MPa	2.75 ± 0.21	1.64 ± 0.15	1.04 ± 0.13	5.24 ± 0.24	7.83 ± 0.26	6.79 ± 0.23
Elongation at break, %	664 ± 43	542 ± 42	215 ± 34	1019 ± 76	570 ± 47	887 ± 63
Tensile strength at 25%, MPa	0.25 ± 0.01	0.23 ± 0.01	0.40 ± 0.01	0.46 ± 0.01	0.65 ± 0.01	0.88 ± 0.01
Tensile strength at 100%, MPa	0.53 ± 0.02	0.50 ± 0.01	0.68 ± 001	0.79 ± 0.01	1.05 ± 0.01	1.57 ± 0.02
Tensile strength at 300%, MPa	0.79 ± 0.02	0.85 ± 0.02	—	1.19 ± 0.03	1.80 ± 0.04	2.38 ± 0.04
At 180 °C						
Tensile strength, MPa	0.23 ± 0.01	0.44 ± 0.01	0.54 ± 0.02	0.70 ± 0.03	0.72 ± 0.03	0.74 ± 0.03
Elongation at break, %	11 ± 1.2	54 ± 1.5	79 ± 2.1	100 ± 2.9	100 ± 2.8	95 ± 2.9
Tensile strength at 25%, MPa	—	0.31 ± 0.01	0.33 ± 0.01	0.39 ± 0.01	0.41 ± 0.02	0.41 ± 0.01
Tensile strength at 100%, MPa	—	—	0.15 ± 0.01	0.70 ± 0.02	0.63 ± 0.02	—

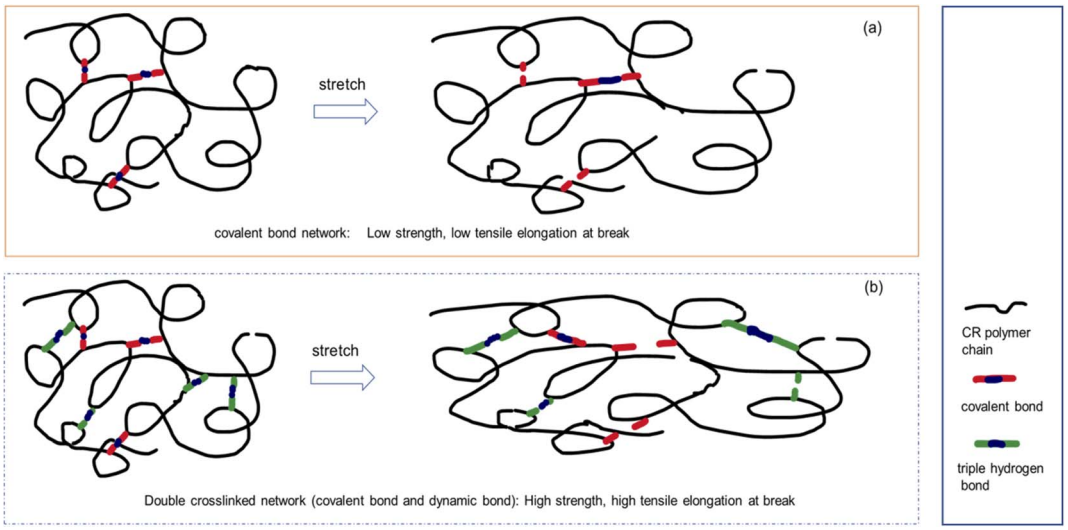

Fig. 5 Schematic diagram of the tensile mechanism of single-network and double-network cross-linked CR. (a) Covalent bond network, (b) double crosslinked network.

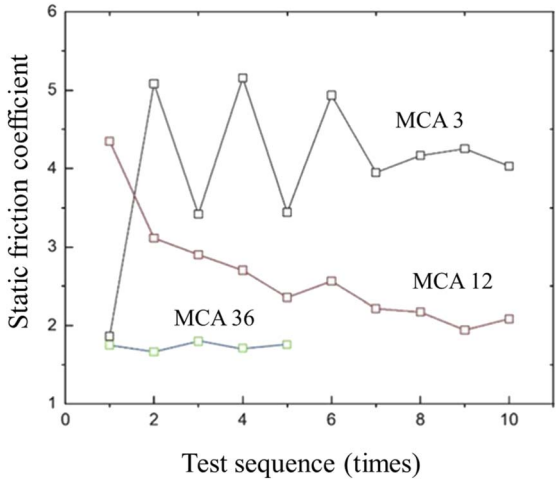

Fig. 6 Relationship of coefficient of static friction and test sequence for CR/MCA vulcanizates.

tested many times. It was found in the test that the static coefficient of friction (SCOF) of CR vulcanizate without MCA could not be measured. As shown in Fig. 6, when the MCA content is 3–12 wt%, the SCOF of CR/MCA vulcanizate fluctuates significantly. The static friction coefficient tends to decrease with the increase of the number of tests. The possible reason is that, with the increase of the number of tests, CR content on the CR/MCA vulcanizate surface gradually decreases, while MCA content increases (confirmed by IR results), which is conducive to the stability of the test data.

The median and average data of the dynamic coefficient of friction and static coefficient of friction (SCOF) of CR/MCA vulcanizate are shown in Table 4. With the increase of MCA content, both the dynamic friction coefficient and the static friction coefficient gradually decreased, indicating that MCA can effectively reduce the friction coefficient of CR/MCA vulcanizate.

3.5 The effect of MCA on the limiting oxygen index of CR/MCA

CR vulcanizate usually has good flame-retardant properties and is frequently used in conditions with fire protection requirements. However, when it is used in conditions with high fire protection requirements, the limit oxygen index (LOI) of CR vulcanizate usually cannot meet the requirements of the index. The initial purpose of this paper is to improve CR flame retardant properties. IR and tensile properties of CR/MCA prove that MCA do react with CR, so it is particularly important to investigate the flame-retardant properties of MCA to CR.

The flame-retardant mechanism of MCA is related to the inert gas (diluted oxygen) generated by thermal decomposition,

Table 4 Median and average of SCOF and DCOF test data for CR/MCA vulcanizates

	Sample					
Test items	C-M0	C-M3	C-M6	C-M12	C-M24	C-M36
Median date of SCOF	—	4.10 ± 0.32	2.09 ± 0.23	2.46 ± 0.25	2.11 ± 0.23	1.75 ± 0.22
Average date of SCOF	—	4.03 ± 0.34	2.12 ± 0.25	2.64 ± 0.22	2.11 ± 0.26	1.74 ± 0.21
Median date of DCOF	—	1.66 ± 0.19	1.38 ± 0.15	1.52 ± 0.18	1.43 ± 0.17	1.37 ± 0.15
Average date of DCOF	—	1.58 ± 0.17	1.39 ± 0.14	1.53 ± 0.13	1.43 ± 0.18	1.39 ± 0.16

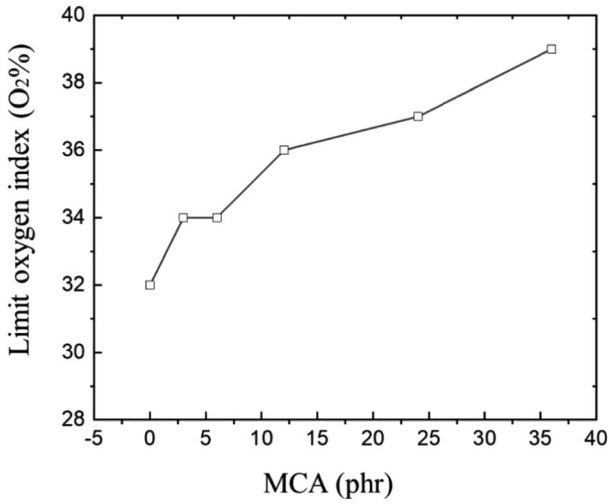

Fig. 7 Limiting oxygen index of CR/MCA vulcanizates.

the generated expansion insulation layer and nitrogen oxides (to capture the free radicals and terminate the combustion reaction).[43,44] It can be seen from Fig. 7, with the increase of MCA content, the LOI of CR/MCA vulcanizate continuously increases from 32 to 39, indicating that MCA (although MCA has reacted with CR) can effectively improve the flame retardancy of CR/MCA.

4 Conclusions

In this study, it was found for the first time that MCA can act as a reactive flame retardant for CR. Cyanuric acid of MCA reacts with chloroprene rubber to graft cyanuric acid onto the molecular chain of CR under the catalysis of base; the cyanuric acid hanging on the side chain can interact with melamine molecules (locate at the MCA interface) to form triple H-bonding crosslinks. Since the rubber also contains zinc oxide, two types of crosslinking networks are formed in the vulcanizate, namely the traditional covalent bond crosslinking network and the dynamic triple H-bonding crosslinking network. The triple H-bonding crosslinks can dynamically dissociate and recombine, thus achieving a simultaneous increase of tensile strength and elongation at break. The tensile strength of C-M36 vulcanizate is 2.5 times that of zinc oxide cross-linked C-M0 vulcanizate, while the elongation at break of C-M36 vulcanizate is 1.3 times that of zinc oxide cross-linked C-M0 vulcanizate. At the same time, the LOI of C-M36 increases from 32% to 39%. This research is of great significance for expanding the application scenarios of CR.

Conflicts of interest

There are no conflicts to declare.

Notes and references

1 P. R. Johnson, Polychloroprene rubber, *Rubber Chem. Technol.*, 1976, **49**(3), 650–702.
2 Y. A. Treger, K. A. Morozov, G. S. Dasaeva, *et al*, Chloroprene rubber: application and production, *Fine Chem. Technol.*, 2018, **13**(4), 26–38.
3 J. Hui, Z. Dong, Y. Shi, *et al.*, Reversible-deactivation radical polymerization of chloroprene and the synthesis of novel polychloroprene-based block copolymers by the RAFT approach, *RSC Adv.*, 2014, **4**(98), 55529–55538.
4 J. Hui, Y. Shi, T. Li, *et al.*, Reverse iodine transfer polymerization (RITP) of chloroprene, *RSC Adv.*, 2015, **5**(55), 44326–44335.
5 A. Das, F. R. Costa, U. Wagenknecht, *et al.*, Nanocomposites based on chloroprene rubber: effect of chemical nature and organic modification of nanoclay on the vulcanizate properties, *Eur. Polym. J.*, 2008, **44**(11), 3456–3465.
6 Z. Xu, L. Zheng, S. Wen, *et al.*, Graphene oxide-supported zinc oxide nanoparticles for chloroprene rubber with improved crosslinking network and mechanical properties, *Composites, Part A*, 2019, **124**, 105492.
7 H. P. Xiang, M. Z. Rong and M. Q. Zhang, Self-healing, reshaping, and recycling of vulcanized chloroprene rubber: A case study of multitask cyclic utilization of cross-linked polymer, *ACS Sustainable Chem. Eng.*, 2016, **4**(5), 2715–2724.
8 B. P. Kapgate, C. Das, A. Das, *et al.*, Reinforced chloroprene rubber by in situ generated silica particles: Evidence of bound rubber on the silica surface, *J. Appl. Polym. Sci.*, 2016, **133**(30), 43717.
9 L. Kong, Y. Zhu, G. Huang, *et al.*, Carbon nanodots as dual role of crosslinking and reinforcing chloroprene rubber, *Compos. Commun.*, 2020, **22**, 100441.
10 M. G. Maya, S. C. George, T. Jose, *et al.*, Development of a flexible and conductive elastomeric composite based on chloroprene rubber, *Polym. Test.*, 2018, **65**, 256–263.
11 C. A. Stewart Jr and U. Staff, Chloroprene[J], *Kirk-Othmer Encycl. Chem. Technol.*, 2000, 1–9.
12 I. K. Sung and C. Y. Park, Fire resistance properties of chloroprene rubber containing inorganic flame retardant, *Elastomers Compos.*, 2015, **50**(4), 279–285.
13 W. Yuan, H. Chen, R. Chang, *et al.*, Synthesis and characterization of NaA zeolite particle as intumescent flame retardant in chloroprene rubber system, *Particuology*, 2011, **9**(3), 248–252.
14 A. Sacco, F. Bella, S. De La Pierre, *et al.*, Electrodes/Electrolyte Interfaces in the Presence of a Surface-Modified Photopolymer Electrolyte: Application in Dye-Sensitized Solar Cells, *ChemPhysChem*, 2015, **16**(5), 960–969.
15 F. Bella, E. D. Ozzello, S. Bianco, *et al.*, Photo-polymerization of acrylic/methacrylic gel–polymer electrolyte membranes for dye-sensitized solar cells, *Chem. Eng. J.*, 2013, **225**, 873–879.
16 L. Wang, F. Zhang, T. Liu, *et al.*, A crosslinked polymer as dopant-free hole-transport material for efficient n-i-p type perovskite solar cells, *J. Energy Chem.*, 2021, **55**, 211–218.
17 F. Bella, E. D. Ozzello, A. Sacco, *et al.*, Polymer electrolytes for dye-sensitized solar cells prepared by photopolymerization of PEG-based oligomers, *Int. J. Hydrogen Energy*, 2014, **39**(6), 3036–3045.

18 A. R. Tripathy, P. K. Patra, J. K. Sinha, *et al.*, Application of differential scanning calorimetry and differential thermogravimetry techniques to determine the ratio of blend components in reactive chlorinated elastomer blends, *J. Appl. Polym. Sci.*, 2002, **83**(5), 937–948.
19 P. Kovacic, Bisalkylation Theory of Neoprene Vulcanization, *Ind. Eng. Chem.*, 1955, **47**(5), 1090–1094.
20 X. Wang, S. Yu and H. Liu, *A Novel Neoprene Vulcanization Method*, CN107365439A, 2017.
21 C. H. Li, C. Wang, C. Keplinger, *et al.*, A highly stretchable autonomous self-healing elastomer, *Nat. Chem.*, 2016, **8**(6), 618–624.
22 C. Y. Shi, Q. Zhang, C. Y. Yu, *et al.*, An Ultrastrong and Highly Stretchable Polyurethane Elastomer Enabled by a Zipper-Like Ring-Sliding Effect, *Adv. Mater.*, 2020, **32**(23), 2000345.
23 J. H. Xu, W. Chen, C. Wang, *et al.*, Extremely stretchable, self-healable elastomers with tunable mechanical properties: synthesis and applications, *Chem. Mater.*, 2018, **30**(17), 6026–6039.
24 Y. Wang, Q. Chen, G. Zhang, *et al.*, Polyimide/ZnO composite cooperatively crosslinked by Zn^{2+} salt-bondings and hydrogen bondings for ultraflexible organic solar cells, *Chem. Eng. J.*, 2023, **451**, 138612.
25 T. Chen, K. Geng, Y. Gao, *et al.*, Highly stretchable and strong poly (butylene maleate) elastomers via metal–ligand interactions, *Polym. Chem.*, 2021, **12**(6), 893–902.
26 M. Zhong, Y. T. Liu and X. M. Xie, Self-healable, super tough graphene oxide–poly (acrylic acid) nanocomposite hydrogels facilitated by dual cross-linking effects through dynamic ionic interactions, *J. Mater. Chem. B*, 2015, **3**(19), 4001–4008.
27 U. Braun and B. Schartel, Flame retardancy mechanisms of aluminium phosphinate in combination with melamine cyanurate in glass-fibre-reinforced poly (1, 4-butylene terephthalate), *Macromol. Mater. Eng.*, 2008, **293**(3), 206–217.
28 M. Zhao, D. Yi, G. Camino, *et al.*, Interdigitated crystalline MMT–MCA in polyamide 6, *RSC Adv.*, 2017, **7**(2), 861–869.
29 J. Cai, A. Wirasaputra, Y. Zhu, *et al.*, The flame retardancy and rheological properties of PA6/MCA modified by DOPO-based chain extender, *RSC Adv.*, 2017, **7**(32), 19593–19603.
30 S. Fan, R. Yuan, D. Wu, *et al.*, Silicon/nitrogen synergistically reinforced flame-retardant PA6 nanocomposites with simultaneously improved anti-dripping and mechanical properties, *RSC Adv.*, 2019, **9**(14), 7620–7628.
31 Y. Nagasawa, M. Hotta and K. Ozawa, Fast thermolysis/FT-IR studies of fire-retardant melamine-cyanurate and melamine-cyanurate containing polymer, *J. Anal. Appl. Pyrolysis*, 1995, **33**, 253–267.
32 A. G. Bielejewska, C. E. Marjo, L. J. Prins, *et al.*, Thermodynamic stabilities of linear and crinkled tapes and cyclic rosettes in melamine–cyanurate assemblies: a model description, *J. Am. Chem. Soc.*, 2001, **123**(31), 7518–7533.
33 H. Jiang, M. Bi, D. Ma, *et al.*, Flame suppression mechanism of aluminum dust cloud by melamine cyanurate and melamine polyphosphate, *J. Hazard. Mater.*, 2019, **368**, 797–810.
34 H. Huang, K. Zhang, J. Jiang, *et al.*, Highly dispersed melamine cyanurate flame-retardant epoxy resin composites, *Polym. Int.*, 2017, **66**(1), 85–91.
35 L. M. A. Perdigão, N. R. Champness and P. H. Beton, Surface self-assembly of the cyanuric acid–melamine hydrogen bonded network, *Chem. Commun.*, 2006, (5), 538–540.
36 Y. Bayat and F. Hajighasemali, Synthesis and characterization of 1, 3, 5-tris ((1/2H-tetrazol-5-yl) methyl)-1, 3, 5-triazinane-2, 4, 6-trione, *Chem. Pap.*, 2017, **71**(5), 949–952.
37 M. Mascal, I. Yakovlev, E. B. Nikitin, *et al.*, Fluoride-selective host based on anion–π interactions, ion pairing, and hydrogen bonding: synthesis and fluoride-ion sandwich complex, *Angew. Chem., Int. Ed.*, 2007, **46**(46), 8782–8784.
38 P. Meng, A. Brock, Y. Xu, *et al.*, Crystal Transformation from the Incorporation of Coordinate Bonds into a Hydrogen-Bonded Network Yields Robust Free-Standing Supramolecular Membranes, *J. Am. Chem. Soc.*, 2020, **142**(1), 479–486.
39 J. Xia, N. Karjule, B. Mondal, *et al.*, Design of melem-based supramolecular assemblies for the synthesis of polymeric carbon nitrides with enhanced photocatalytic activity, *J. Mater. Chem. A*, 2021, **9**(33), 17855–17864.
40 Z. Sun, W. Wang, Q. Chen, *et al.*, A hierarchical carbon nitride tube with oxygen doping and carbon defects promotes solar-to-hydrogen conversion, *J. Mater. Chem. A*, 2020, **8**(6), 3160–3167.
41 Z. Tang, X. Wu, B. Guo, *et al.*, Preparation of butadiene–styrene–vinyl pyridine rubber–graphene oxide hybrids through co-coagulation process and in situ interface tailoring, *J. Mater. Chem. A*, 2012, **22**(15), 7492–7501.
42 N. V. Salim, N. Hameed and Q. Guo, Competitive hydrogen bonding and self-assembly in poly(2-vinyl pyridine)-block-poly(methyl methacrylate)/poly(hydroxyether of bisphenol A) blends, *J. Polym. Sci., Part B: Polym. Phys.*, 2009, **47**(19), 1894–1905.
43 Y. Liu and Q. Wang, The investigation on the flame retardancy mechanism of nitrogen flame retardant melamine cyanurate in polyamide 6, *J. Polym. Res.*, 2009, **16**(5), 583–589.
44 W. Chen, P. Liu, Y. Cheng, *et al.*, Flame retardancy mechanisms of melamine cyanurate in combination with aluminum diethylphosphinate in epoxy resin, *J. Appl. Polym. Sci.*, 2019, **136**(12), 47223.